

pubs.acs.org/est Article

Photoproduction Rates of One-Electron Reductants by Chromophoric Dissolved Organic Matter via Fluorescence Spectroscopy: Comparison with Superoxide and Hydrogen Peroxide Rates

Danielle M. Le Roux, Leanne C. Powers, and Neil V. Blough*



Cite This: Environ. Sci. Technol. 2021, 55, 12095-12105



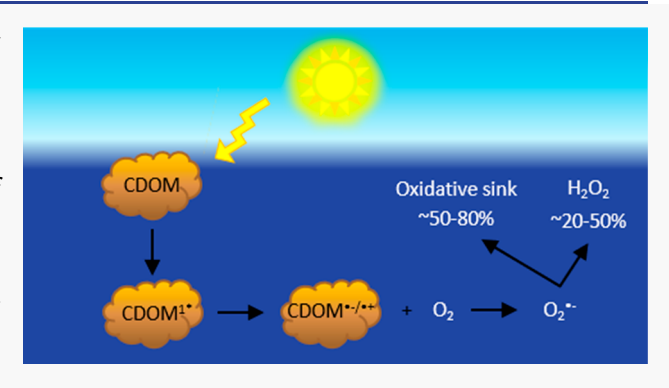
ACCESS I

III Metrics & More

Article Recommendations

SI Supporting Information

ABSTRACT: One-electron reductants (OER) photoproduced by chromophoric dissolved organic matter (CDOM) have been shown to be likely precursors for the formation of superoxide and subsequently hydrogen peroxide. An improved method that employs a nitroxide radical probe (3AP) has been developed and utilized to determine the photoproduction rates of OER from a diverse set of CDOM samples. 3AP reacts with OER to produce the hydroxylamine, which is then derivatized with fluorescamine and quantified spectrofluorometrically. Although less sensitive than traditional methods for measuring $R_{\rm O2\bullet-}$, measuring $R_{\rm H}$ provides a simpler and faster method of estimating $R_{\rm O2\bullet-}$ and is amenable to continuous measurement via flow injection analysis. Production rates of OER $(R_{\rm H})$, superoxide $(R_{\rm O2\bullet-})$, and hydrogen peroxide



 $(R_{\rm H2O2})$ have a similar wavelength dependence, indicating a common origin. If all the OER react with molecular oxygen to produce superoxide, then the simplest mechanism predicts that $R_{\rm H}/R_{\rm H2O2}$ and $R_{\rm O2\bullet-}/R_{\rm H2O2}$ should be equal to 2. However, our measurements reveal $R_{\rm H}/R_{\rm H2O2}$ values as high as 16 (5.7–16), consistent with prior results, and $R_{\rm O2\bullet-}/R_{\rm H2O2}$ values as high as 8 (5.4–8.2). These results indicate that a substantial fraction of superoxide (65–88%) is not undergoing dismutation. A reasonable oxidative sink for superoxide is reaction with photoproduced phenoxy radicals within CDOM.

KEYWORDS: quantum yields, optical properties, oxidative sink, photooxidation

INTRODUCTION

Chromophoric dissolved organic matter (CDOM) is the lightabsorbing component of dissolved organic matter (DOM), which is found ubiquitously in natural waters. Although some fraction of CDOM may be consumed, transformed, or transported into sediments, a large portion remains in the water column where it plays important roles in the aquatic environment.1 Photoactive groups within CDOM absorb light to produce excited states that undergo photochemistry to generate reactive oxygen species (ROS) such as superoxide, hydrogen peroxide, singlet oxygen, and hydroxyl radicals.²⁻ ROS are environmentally significant species as they affect trace metal speciation through redox chemistry, which can affect the bioavailability of these metals. 5-7 ROS can also contribute to the transformation of natural and anthropogenic organic compounds.8-13 Studying the rates and mechanisms of formation and decay of these ROS is thus essential to acquire a better understanding of the impact these ROS have on aquatic ecosystems.

A previously proposed series of reactions, shown in Scheme 1, for the generation of superoxide and hydrogen peroxide

Scheme 1. Proposed Reactions Involved in the Generation of ROS from CDOM upon Absorption of Light

$$\begin{split} &1. \ CDOM + hv \rightarrow {}^{1}CDOM^{*}\\ &2. \ {}^{1}CDOM^{*} \rightarrow CDOM^{D\bullet + / A\bullet -}\\ &3. \ CDOM^{D\bullet + / A\bullet -} + O_{2} \rightarrow CDOM^{D\bullet + / A} + O_{2}^{\bullet -}\\ &4. \ CDOM^{D\bullet + / A\bullet -} \rightarrow CDOM^{D/A}\\ &5. \ 2O_{2}^{\bullet -} + 2H^{+} \rightarrow H_{2}O_{2} + O_{2} \end{split}$$

involves an initial absorption of light $(h\nu)$, resulting in the formation of excited singlet states ($^{1}\text{CDOM*}$) (Reaction 1).^{4,14} On the basis of current evidence, intramolecular electron transfer then occurs between electron-rich donors (D) and electron-poor acceptors (A) within CDOM, where

Received: June 21, 2021 Revised: August 2, 2021 Accepted: August 4, 2021 Published: August 12, 2021





possible donors are likely to be phenols while possible acceptors are quinones or aromatic ketones. 15,16 The electron transfer results in the formation of one-electron reduced acceptors within CDOM (CDOM $^{D\bullet+/A\bullet-}$), which then react with dissolved molecular oxygen to form superoxide ($O_2^{\bullet-}$) (Reaction 3). This reaction takes place in competition with back-electron transfer (Reaction 4). Superoxide then undergoes dismutation to form hydrogen peroxide (H_2O_2) (Reaction 5). $^{17-19}$

On the basis of this reaction scheme, the ratio of the production rate of superoxide to that of hydrogen peroxide should be equal to 2, as it takes two superoxide molecules to produce one hydrogen peroxide. However, past research is inconsistent with these values and suggests that oxidative sinks for superoxide are present that do not lead to hydrogen peroxide production. 15 Previously, the enzyme superoxide dismutase (SOD) has been utilized to enhance hydrogen peroxide production in water samples by catalyzing the dismutation of superoxide $(2 \times 10^9 \text{ M}^{-1} \text{ s}^{-1})^{20}$ and thereby outcompeting other decay pathways. Using this approach, Petasne and Zika discovered that up to 41% of the superoxide generated in coastal seawater samples does not dismutate to form hydrogen peroxide. 19 Powers et al. 21 combined the use of SOD with superoxide measurements and also obtained a discrepancy of about 40% for natural freshwater from the Altamaha River and seawater samples from the Skidaway River Estuary and the South Atlantic Bight. Garg et al. monitored hydrogen peroxide production in Suwannee River fulvic acid samples in the presence of SOD and showed that the loss of superoxide to other pathways was at least 70%.²² However, SOD was found to have no effect on hydrogen peroxide production in several other studies.^{23,24}

The proposed precursor to superoxide, photoproduced OER, have been found to react rapidly with nitroxide radical probes to reduce them to form the relatively stable Ounsubstituted hydroxylamine. 15,25 Derivatization of the hydroxylamine with fluorescamine leads to a product with enhanced fluorescence, while derivatization of the nitroxide radical probe (prior to being reduced) has very low fluorescence due to efficient intramolecular quenching by the nitroxide moiety.²⁶⁻²⁸ Liquid chromatography with fluorescence detection has been employed to separate and quantify photoproduced radicals through irradiation of various α -keto acids and ketones and of reference materials and natural waters, ^{29,30} with the structures confirmed using mass spectrometry. ^{31,32} Irradiation of Suwannee River fulvic acid (SRFA) and natural waters led to the production of a variety of compounds including the hydroxylamine, as well as much smaller levels of methyl, ethyl, isopropyl, acetyl, propanoyl, and pentanoyl adducts. 29,32 The hydroxylamine was found to dominate the products generated as compared to the formation of radical adducts. 29,32

Because the hydroxylamine is the major product, its steady-state fluorescence signal should dominate compared to the very small contributions from other products, making separation unnecessary. Therefore, the nitroxide probe and derivatization method was modified to be conducted simply using fluorescence spectroscopy to quantify the production of OER $(R_{\rm H})$ photoproduced within CDOM. Assuming that $R_{\rm H}$ is approximately equal to the production of superoxide $(R_{\rm O2\bullet-})$, a comparison of $R_{\rm H}$ to the production rate of hydrogen peroxide $(R_{\rm H2O2})$ should also produce ratios of about 2. Prior work using liquid chromatography that compared $R_{\rm H}$

to $R_{\rm H2O2}$ for standard humic and fulvic materials from the Suwannee River discovered much higher values, some reaching up to 13. ¹⁵

This work presents a faster and more versatile method for the measurement of $R_{\rm H}$, provides further tests of the validity of the method, and acquires results for a broader range of samples compared to previous studies. Validation experiments are consistent with previously published results 25,25 and include: (1) nitroxide probe, fluorescamine, and CDOM concentration dependence; (2) linearity of production over time; (3) stability in air; (4) oxidation of the hydroxylamine by copper; and (5) detection limits. R_H values have been determined for Suwannee River fulvic acid (SRFA) and natural organic matter (SRNOM), Elliott Soil humic acid (ESHA), exudate from the brown alga Sargassum natans, a natural water and extract (C-18 solid phase) from the Delaware River, natural waters from various lakes in New Jersey, and a natural water and extract from St. Mary's River in Maryland. RH were compared with $R_{\rm H2O2}$ and all samples exhibited ratios far greater than 2, in accordance with past results. 15 Salinity and the addition of a metal chelator have only a slight impact on these ratios. To delve deeper into the relationship between the reactions in Scheme 1, preliminary work acquired $R_{O2\bullet-}$ for SRFA and SRNOM. Presented herein are the first measurements of the production rates of all three species under identical conditions, as well as the first direct measurements of the polychromatic wavelength dependence of $R_{O2\bullet-}$ using multiple long-pass cutoff filters.

MATERIALS AND METHODS

Chemicals. Boric acid, sodium carbonate, sodium acetate, monobasic sodium phosphate, sodium hydroxide, phosphoric acid, sea salt (\$9883), fluorescamine, 3-amino-2,2,5,5-tetramethyl-1-pyrrolidinyloxy (3AP), and 0.1 N potassium permanganate were purchased from Millipore Sigma. Sodium dithionite was purchased from Acros Organics. Hydrogen peroxide and sodium chloride were purchased from EMD. Acetonitrile, acetone, and ethanol were purchased from Fischer. 10-Methyl-9-(p-formylphenyl) acridinium carboxylate trifluoromethanesulfonate (AE) was obtained from Waterville Analytical Co. 2-Methyl-6-(4-methoxyphenyl)-3,7dihydroimidazo[1,2-a]pyrazin-3(7H)-one) (also known as methyl Cypridina luciferin analogue or MCLA) was purchased from TCI Chemicals. Diethylenetriaminepentaacetic acid (DTPA) was purchased from Fluka. Suwannee River fulvic acid (SRFA; 2S101F), Suwannee River natural organic matter (SRNOM; 2R101N), Elliott soil humic acid (ESHA; 1S102H) were purchased from the International Humic Substance Society. Sargassum was sampled in the North Atlantic Ocean, 9 km off the coast of Bermuda, and exudates were collected by solid phase extraction during outdoor leaching experiments described in detail previously.³³ Natural water (NW) from the Delaware River was collected in August of 2006 (St. Nineteen; 40.1 N, -74.8 W). Natural waters from various lakes in northern New Jersey were collected in November and December of 2019: Echo Lake Reservoir (ECL; 41.0, -74.4), Greenwood Lake (GWL; 41.2, -74.4) and Monksville Reservoir (MKR; 41.1, -74.3). Natural water from St. Mary's River in Maryland was collected in January of 2020 (SMR; 38.2, -76.5). All C-18 solid phase extractions (EX) were conducted as described previously.³⁴ Purified water (18 $M\Omega$ cm) was obtained from a Milli-Q purification system.

Sample Preparation. Stock solutions of extracts and reference materials were prepared by diluting/dissolving the extract or reference material in MQ water. These stocks were adjusted to pH 7 using NaOH and HCl and filtered using precleaned 0.2 μ M nylon filters. Dilutions of these stocks at desired concentrations for experiments were then prepared by diluting the stock solutions with 50 mM borate buffer at a pH of 8 unless otherwise noted. Natural waters were filtered with precleaned 0.2 μ m nylon filters and used as is.

Measurement of Optical Properties. Absorbance measurements were conducted on a Shimadzu UVPC 2401 benchtop spectrophotometer in a 1 cm cell. The instrument was always baselined to air and blank measurements (MQ or buffer) were taken and were subtracted from absorbance spectra. Spectral slopes were determined using nonlinear least-squares fitting to an exponential function in SigmaPlot.

Fluorescence excitation—emission spectra (EEMs) were conducted with a Horiba Fluoromax-4. Excitation was scanned from 300 to 500 nm every 10 nm, and the emission was scanned from 300 to 700 nm every 1 nm. Band passes were 4 nm and the integration time was 0.2 s. First and second order Rayleigh masking settings were used. The fluorescence of 10 ppb quinine sulfate in 1 N $\rm H_2SO_4$ (QS) was measured using an excitation wavelength of 350 nm with emission scanned from 290 to 700 nm. Fluorescence quantum yields (FQY) at any given excitation wavelength for the samples were calculated using the following equation: 35

$$FQY(\lambda_{ex}) = \left(\frac{F_{s(int)}(\lambda_{ex})}{F_{QS(int)}(\lambda_{ex_{350nm}})} \times \frac{A_{QS}(\lambda_{ex_{350nm}})}{A_{s}(\lambda_{ex})}\right) \times 0.51$$
(1)

where $F_{s(int)}$ and $F_{QS(int)}$ are the integrated emission intensities of the sample and QS, respectively, at the particular excitation wavelength (λ_{ex}) . A_{QS} and A_s are the absorbance values of QS and the sample, respectively. The value 0.51 is the published quantum yield of QS.³⁵

Measurement of One-Electron Reductants (Hydroxylamine). The production of OER ($R_{\rm H}$) was measured using 3-amino-2,2,5,5-tetramethyl-1-pyrrolydinyloxy (3AP) followed by derivatization with fluorescamine. Fluorescence measurements were conducted with a Horiba Fluoromax-4. The excitation wavelength was set to 450 nm, band passes were 4 nm, the integration time was 0.1 s, and the emission was scanned from 460 to 600 nm. Although 390 nm is approximately the wavelength of maximum absorption, an excitation wavelength of 450 nm was used to prevent inner filter effects and to reduce the background due to CDOM itself. The emission intensity at 490 nm was used for data analysis.

A standard curve for hydroxylamine was produced by titrating 600 μ M 3AP with increasing volumes of dithionite (Na₂S₂O₄) under nitrogen and observing the emission with each addition (Figure S1 of the Supporting Information, SI).²⁹ Dithionite was prepared by adding a small amount of the solid to a cuvette of Milli-Q water at pH 11 that had been deoxygenated. The concentration of the resulting dithionite solution was monitored spectrophotometrically (ε = 8000 M⁻¹cm⁻¹ at 315 nm).³⁶ Standard curves were performed in at least triplicate.

Unless otherwise noted, samples were mixed with 600 μ M 3AP in 1 cm screw-top cuvettes fitted with caps and septa to measure $R_{\rm H}$. Nitrogen was first bubbled through the sample for

30 min and was then irradiated for 15 min using a 300-W xenon arc lamp with a 20 cm water jacket. A 325 nm cutoff was the primary filter used to approximate the solar spectrum in natural waters, but other filters (355, 380, 399, 418, and 440 nm) were used to examine the wavelength dependence of $R_{\rm H}$. The headspace of the cuvette was continuously purged with nitrogen throughout the irradiation. The sample was then derivatized directly in the cuvette, using anoxic techniques, by the addition of 200 μ L of 15 mM fluorescamine in acetonitrile (1 mM in sample) unless otherwise noted. The sample was mixed for about one minute and was then placed in the fluorometer for measurement. A nonirradiated sample was derivatized and measured to determine the blank. If necessary, samples were then filtered with a precleaned 0.2 μ m nylon filter into a clean cuvette to remove any excess precipitated fluorescamine, and the fluorescence was measured. Filtering the samples removes issues with scattering in the measurements and does not remove any of the hydroxylamine product (Figure S2). The initial rate of hydroxylamine production was calculated by the following equation:

$$R_{\rm H} = \frac{T_{15} - T_0}{15 \, \text{min} \times 60 \, \text{s/min}} \tag{2}$$

where T_{15} is the product yield after the 15 min irradiation, and T_0 is the blank measurement.¹⁵

The hydroxylamine method required some modifications to be used in natural waters due to their variability. Additional buffering of natural waters was needed following irradiation but before derivatization to maintain a higher stable pH and a higher concentration of fluorescamine was needed to ensure complete derivatization. For the natural waters tested in this study, an addition of $\sim \! 100~\mu L$ of a 50 mM borate buffer at pH 11 and 2 mM fluorescamine was sufficient (Text S1).

Measurement of Hydrogen Peroxide. Hydrogen peroxide was measured through the chemiluminescent reaction with a FeLume (Waterville Analytical Co.). For freshwater and buffered samples, the carrier was 0.1 M HCl, the buffer was 0.1 M sodium carbonate at a pH of 11.7, and the reagent acridinium ester (10-methyl-9-(p-formylphenyl) acridinium carboxylate trifluoromethanesulfonate) (AE) was prepared at $5 \mu M$ in 1 mM phosphate buffer at a pH of $3.^{37,38}$ For higher salinity samples, the HCl carrier was increased to 0.3 M, the pH of the sodium carbonate buffer was lowered to 10.7, and the AE concentration was lowered to $1-2 \mu M$. The FIA photomultiplier tube was set at a voltage of 950 V and an integration time of 400 ms for freshwater and buffered samples. The voltage was increased to 1050 V for higher salinity samples. All of these solutions were drawn into the FIA system using a peristaltic pump with Teflon tubing.

Standard concentrations of hydrogen peroxide were prepared from a stock solution whose concentration was monitored spectrophotometrically ($\varepsilon = 38.1 \pm 1.4 \, \mathrm{M^{-1}cm^{-1}}$ at 240 nm). The hydrogen peroxide concentration was confirmed by performing a potassium permanganate titration of the ~30% stock bottle. A concentration of 31.6 \pm 0.2% was obtained. The molar extinction coefficient of hydrogen peroxide was then confirmed by measuring the absorbance of multiple prepared concentrations (Figure S9). An extinction coefficient of 40.4 \pm 0.3 $\mathrm{M^{-1}cm^{-1}}$ (0.5%) at 240 nm was obtained, which differs by 6% compared to the published literature value above.

To determine $R_{\rm H2O2}$, a 1 cm quartz cuvette was filled with the sample, and it was irradiated using the lamp, water jacket,

and filters as describe above. $R_{\rm H2O2}$ was calculated from the linear regression of hydrogen peroxide yield over the course of a 15 min irradiation.

Measurement of Superoxide. Superoxide was measured via the chemiluminescent reaction with 2-methyl-6-(4methoxyphenyl)-3,7-dihydroimidazo[1,2-a]pyrazin-3(7H)one) (also known as methyl Cypridina luciferin analogue or MCLA) in the FeLume system set up to continuously take in the reagent and sample with a peristaltic pump with a total flow rate of 6.6 mL/min. MCLA was prepared at 2.5 μ M in 500 mM sodium acetate buffer with 50 µM DTPA at a pH of 6. 22,40 Standards were generated by the photolysis of a solution of 6 M ethanol, 41 mM acetone, and 30 µM DTPA in 1 mM borate buffer at a pH of about 12.5 in a cuvette with a mercury pen-lamp. 40,41 The concentration of superoxide was monitored spectrophotometrically ($\varepsilon = 2183 \text{ M}^{-1}\text{cm}^{-1}$ at 240 nm)¹⁸ with an Ocean Insight DH mini light source connected to an Ocean Optics USB2000 spectrometer. When the superoxide concentration in the solution reached \sim 50 μ M, a small volume (μ L) was taken and added to ~20 mL of sample to prepare a standard in the nanomolar range. The standards were continuously stirred and taken into the instrument and the signal was monitored as the superoxide decayed. Linear extrapolation of the plot of the natural log of the signal versus time was used to determine what the initial signal was.

To quantify $R_{\rm O2\bullet-}$, about 4 mL of sample was placed in a 1 cm cuvette and the sample line was inserted into the cuvette. The cuvette was placed into the light and the production was monitored over time. Approximately the first 15 s of the observed increase in signal over time was used to calculate $R_{\rm O2\bullet-}$ (Figure S10).

Effect of Salinity. Solutions of 50 mM borate buffer at a pH of 8 with sodium chloride and Sigma-Aldrich "Sea Salt" (S9883) concentrations of 18 and 28 ppt were prepared. St. Nineteen extract samples at concentrations of 5 mg/L were then prepared by bringing up the extract in these buffered salt solutions. $R_{\rm H}$ and $R_{\rm H2O2}$ were then measured as described above. The sodium chloride and sea salt had been baked for 24 h prior to being used to remove any trace organic material. Sonication was done to aid in dissolution, and the salt solutions were filtered through precleaned 0.2 μ M nylon filters before use.

Effect of Metal Chelators. A stock solution of 3.57 mM DTPA was prepared by dissolving the solid in MQ water. Aliquots of the stock were added to St. Nineteen extract and St. Nineteen natural water so that the concentration was 50 μ M and they sat at 4 °C for 24 h. $R_{\rm H}$ and $R_{\rm H2O2}$ were then measured as described above.

Rate of Excitation and Apparent Quantum Yields. Rates of production were normalized to the rate of excitation of the sample to give apparent quantum yields (Φ) .

$$\Phi = \frac{\text{rate of production } (R_{\text{H}}, R_{\text{O2}}, \text{ or } R_{\text{H2O2}})}{\text{rate of excitation } (R_{\text{EX}})}$$
(3)

This ensures that variability in sample concentrations/ absorbance are taken into account. Rate of excitation was calculated under optically thin conditions by the equation:

$$R_{\rm EX} = \int_{300}^{800} a(\lambda)I(\lambda) \, \mathrm{d}\lambda \tag{4}$$

where $a(\lambda)$ is the Naperian absorption coefficient in cm⁻¹, and $I(\lambda)$ is the absolute irradiance of the xenon arc lamp in

photons cm⁻² s⁻¹ nm⁻¹. The absolute irradiance of the lamp from 300 to 800 nm was measured using an Ocean Optics Spectroradiometer (Figure S11).

■ RESULTS AND DISCUSSION

Validation of Hydroxylamine Measurements Using Fluorescence Spectroscopy. The procedure for measuring $R_{\rm H}$, previously conducted using liquid chromatography with fluorescence detection, was modified to allow for determination with a spectrofluorometer. Reduction of 3AP with dithionite to form hydroxylamine, followed by derivatization with fluorescamine, produced an enhanced fluorescence emission that was linear with the extent of reduction of 3AP, thus allowing for method calibration (Figures 1a and S1).

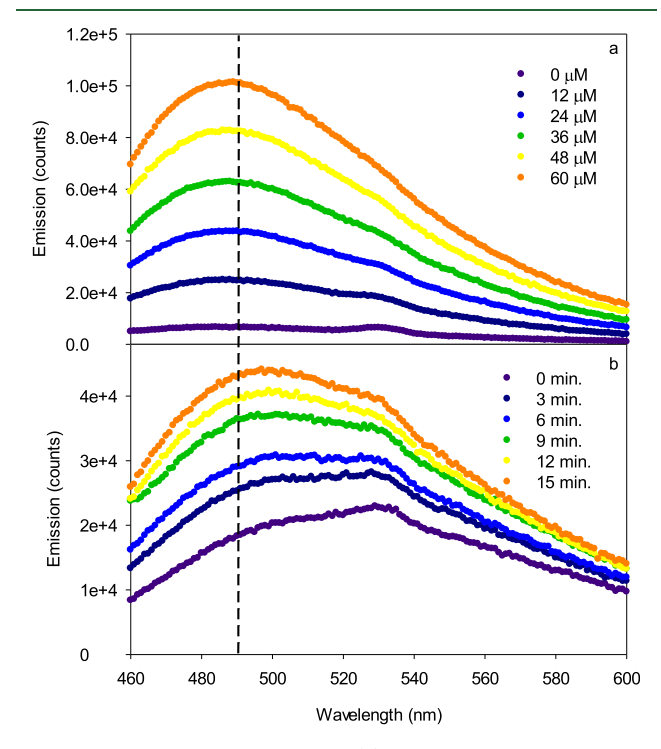


Figure 1. Raw emission signals for (a) hydroxylamine produced via dithionite reduction of $600 \, \mu \text{M}$ 3AP and (b) hydroxylamine produced by reduction of $600 \, \mu \text{M}$ 3AP during an irradiation of $10 \, \text{mg/L}$ SRFA. Dashed line indicates 490 nm, the wavelength at which fluorescence intensity was used for data analysis.

Irradiation of CDOM in the presence of 3AP also produced enhanced signals, indicating reduction of 3AP, which were linear with both the irradiation time (Figures 1b and S12) and the concentration of CDOM (Figure S13). The difference in spectral shape between Figure 1a and Figure 1b is due to the background fluorescence of CDOM. The hydroxylamine signal was stable in air for at least two hours (Figure S14). Introduction of a low concentration (7.3 μ M) of Cu²⁺ reversed this signal, consistent with Cu²⁺-catalyzed oxidation of hydroxylamine back to 3AP^{42,43} and confirming an insignificant contribution of radical adducts (e.g., methyl, acetyl, and pentanoyl)²⁹ to the total fluorescence signal (Figure S15).

To ensure that sufficient 3AP was being utilized to trap all photoproduced OER, the dependence of $R_{\rm H}$ on the concentration of 3AP was evaluated in a solution of 10 mg/L SRFA (Figure 2). Data was fit to eq 5, the derivation of which is discussed in the SI (Text S2).

$$R_{\rm H} = \frac{Ax}{B+x} \tag{5}$$

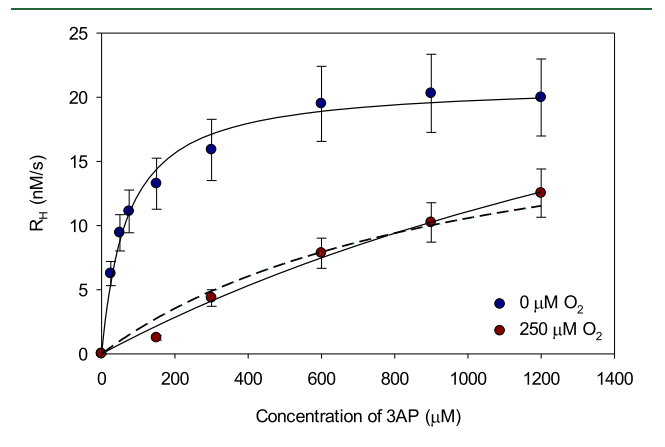


Figure 2. Dependence of $R_{\rm H}$ on 3AP concentration for 10 mg/L SRFA under 0 and 250 $\mu{\rm M}$ molecular oxygen. Irradiations were conducted for 15 min using the 325 nm cutoff filter. Data was fit to eq 5. Solid lines are the fits of the data to eq 5. The dashed line is the fit of the 250 $\mu{\rm M}$ molecular oxygen data to eq 5 but with A restricted to 21.1 nM/s. Error bars are standard deviation based on a relative standard deviation of 15% which was the typical maximum deviation observed for triplicate $R_{\rm H}$ measurements.

The parameter $A=R_{\rm f}$ and parameter $B=\frac{k_{\rm d}+k_{\rm O2}[O_2]}{k_{\rm 3AP}}$. When $[O_2]=0~\mu{\rm M}$ under nitrogen, $B=\frac{k_{\rm d}}{k_{\rm 3AP}}$ and provides the half-saturation concentration for reaction of 3AP with OER.

The data under nitrogen plateaus by 600 μ M, and the resulting fit gave a half-saturation concentration (B) of 70 ± 8 μ M and a rate of formation of OER (A) of 21.1 \pm 0.6 nM/s, somewhat higher than the previously published results of 40 \pm 8 μ M and 16.2 \pm 0.7 nM/s, respectively. 15 We attributed this difference to the broader range of concentrations tested in this iteration, allowing for a better fit than previous results. In the presence of 250 μ M O₂ (estimation based on temperature and solubility), competition between 3AP and molecular oxygen for OER is evidenced by the far lower values obtained for $R_{\rm H}$. For this data, the fit gave $B = 2600 \pm 1200 \,\mu\text{M}$ and $A = 39 \pm$ 13 nM/s; the very large uncertainty we attribute to not reaching rate saturation over the concentration range of 3AP investigated, in accordance with previous results. 15 Restricting the fit with A = 21.1 nM/s (from fit to 0 μ M molecular oxygen) gives $B = 1100 \pm 85 \mu M$, which is more in line with that observed visually for the half-saturation concentration and fits within the expected error of the data. These data provide strong evidence that 3AP and molecular oxygen are competing for the same pool of OER. Further, molecular oxygen and 3AP are highly effective quenchers of both excited singlet and triplet states with rate constants on the order of 10⁹ M⁻¹ s⁻¹ or more,²⁵ primarily via mechanisms not involving electron transfer. These results provide further evidence that the excited states giving rise to the OER must be relatively short-

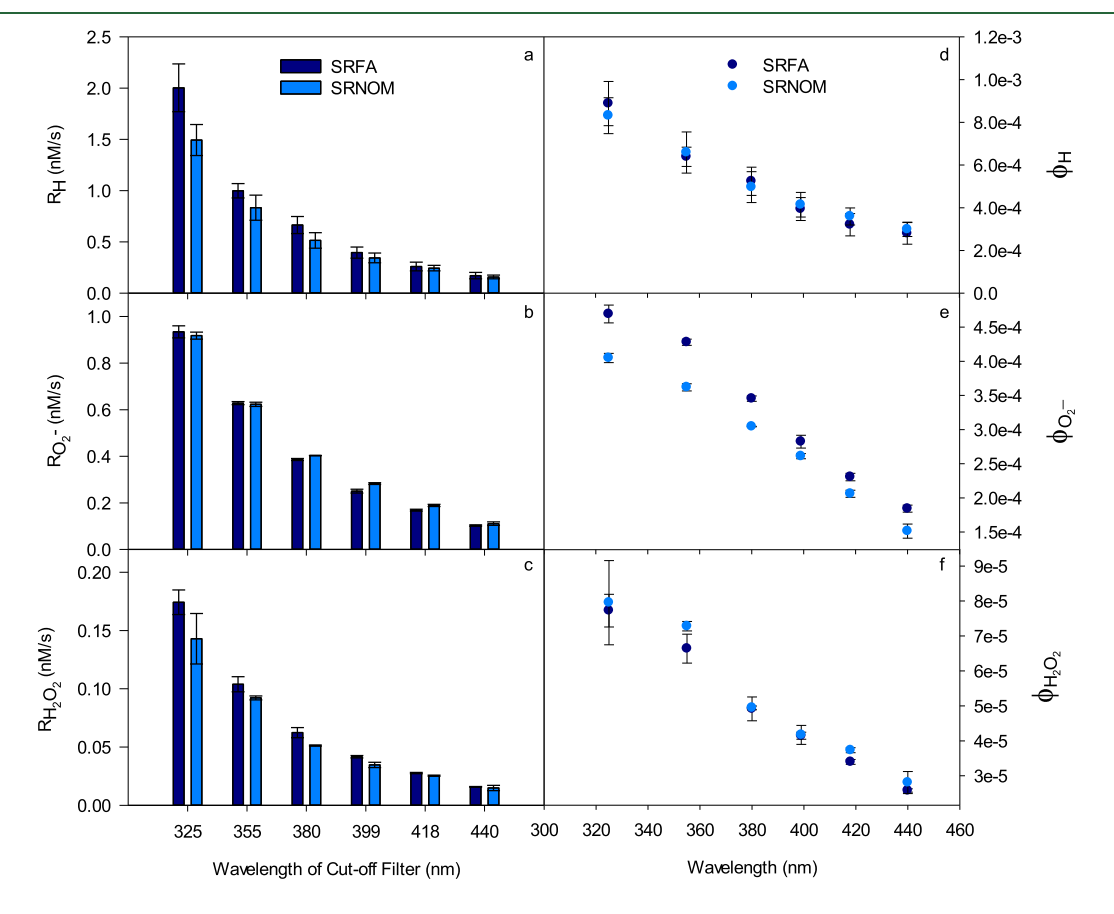


Figure 3. (a) R_{H_2} (b) $R_{O2\bullet-}$, (c) R_{H2O2} , (d) Φ_{H_2} (e) $\Phi_{O2\bullet-}$, and (f) Φ_{H2O2} for 1 mg/L SRFA and SRNOM. Error bars for the rates represent standard deviation of triplicate measurements.

lived and are thus not originating from long-lived triplet states. 25,28,44

The concentration dependence of fluorescamine was also examined to ensure that derivatization of hydroxylamine was complete. This was achieved by irradiating 10 mg/L SRFA in 50 mM borate buffer pH 8 with 600 μ M 3AP for 15 min but varying the concentration of fluorescamine used to derivatize the sample (Figure S16). The emission maximum occurred at 0.8 mM fluorescamine and then plateaued, indicating that 0.8 mM was sufficient to derivatize 600 µM 3AP.

The hydroxylamine technique is quite sensitive and can detect nanomolar concentrations of hydroxylamine (Figure S17). The limit of detection (LOD = 3(s/m)) and the limit of quantification (LOQ = 10 (s/m)) were determined for the hydroxylamine, superoxide, and hydrogen peroxide methods used in this study, where s is the standard deviation of the blank signal, and m is the slope of the standard curve. LOD and LOQ values were determined using at least two standard curves and are reported as the average ± standard deviation. The hydroxylamine method has a LOD of 310 \pm 70 nM and a LOQ of 1000 ± 200 nM. Chemiluminescence methods typically have lower limits, in the picomolar to low nanomolar range. 40,45 In our case, the hydrogen peroxide method had an LOD of 24 \pm 8 nM and a LOQ of 80 \pm 30 nM and the superoxide method had an LOD of 0.4 ± 0.1 nM and an LOQ of 1.2 \pm 0.4 nM. Although the hydroxylamine method is not as sensitive as the superoxide chemiluminescence technique, the simplicity and ease of use of the hydroxylamine method outweigh the loss of sensitivity.

Polychromatic Wavelength Dependence of R_H, R_{O2•-}, and R_{H2O2} . Numerous studies have investigated the wavelength dependence of RH2O2 and have shown that its production decreases approximately exponentially throughout the ultraviolet wavelengths and that there is little to no production in the visible. 46-53,23,54,21 Prior results from limited monochromatic studies have shown that the value for $R_{\rm H}/$ $R_{\rm H2O2}$ is retained despite the wavelength(s) of light used during irradiations. 15,16,55 This work is the first report of $R_{H^{*}}$ $R_{\rm H2O2}$, and $R_{\rm O2\bullet-}$ measurements on the same sample and the first report of the polychromatic wavelength dependence of $R_{O2\bullet-}$ that was acquired directly and not estimated from R_{H2O2}

The wavelength dependence is similar for all three rates (Figure 3); with all decreasing proportionally with longer wavelength cutoff filters. Therefore, specific ranges of wavelengths do not favor R_H, R_{O2•-}, or R_{H2O2} over another. This result further supports that the reactions of the three species are inter-related as described above in Scheme 1. Plots d-f in Figure 3 provide the wavelength dependence of the Φ values. Our results are similar to the few studies that exist for the wavelength dependence of Φ_{H2O2} determined based off of polychromatic irradiations, although our results are toward the lower end of the values. ^{21,23,52,54} This could be attributable to our use of the range of 300-800 nm for integration which is larger than in these studies. Additionally, our results begin with a cutoff filter of 325 nm and most works have studied as low as 280 nm, which is much more photochemically efficient, and these lower wavelengths give the spectra a more exponential

When we relate $R_{O2\bullet-}$ to R_H and R_{H2O2} through ratios (Figure 4), a ratio of about 1-2 is obtained for $R_H/R_{O2\bullet}$ which indicates that superoxide measurements are close in magnitude to those of OER, as expected. The slightly lower $R_{O2\bullet-}$

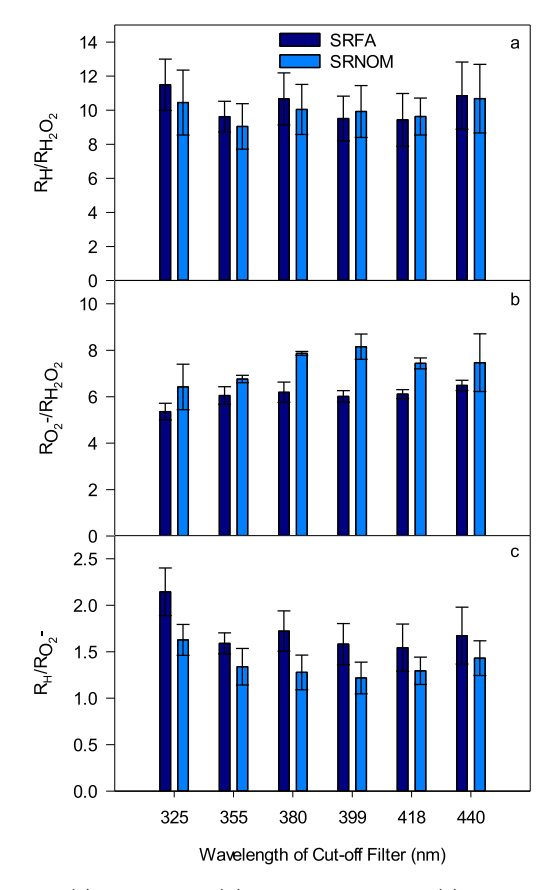


Figure 4. (a) R_H/R_{H2O2} , (b) $R_{O2\bullet-}/R_{H2O2}$ and (c) $R_H/R_{O2\bullet-}$ for SRFA and SRNOM. Error bars represent propagation of standard deviation of triplicate measurements for each rate.

compared to $R_{\rm H}$ could be due to the inability to completely capture an actual production rate of superoxide. The rates reported here are "net" in that some unavoidable loss occurs as the superoxide travels from the sample to the reagent and detector within the FeLume. Alternatively, small systematic variations in the calibration of either $R_{\rm H}$ or $R_{\rm O2 ullet-}$ could be possible, particularly for $R_{O2\bullet-}$ due to the difficult nature of calibrating for superoxide. In contrast, a ratio of about 11 is obtained for $R_{\rm H}/R_{\rm H2O2}$, consistent with previous work, ¹⁵ with a value of about 6-8 obtained for $R_{\rm O2 \bullet -}/R_{\rm H2O2}$, further confirming that $R_{O2\bullet-}$ cannot be simply estimated as 2 \times $R_{\rm H2O2}$, which is what has traditionally been done. ^{21,56}

Comparison of Rates and Φ Values for Different **Samples.** $R_{\rm H}$ and $R_{\rm H2O2}$ were determined for SRFA, SRNOM, ESHA, a natural water and an extract from the Delaware River (St. Nineteen), exudate from Sargassum, natural waters from lakes and reservoirs in northern New Jersey [Echo Lake Reservoir (ECL), Greenwood Lake (GWL) and Monksville Reservoir (MKR)], and a natural water and an extract from St. Mary's River (SMR) in Maryland (Table 1). For all samples, $R_{\rm H}/R_{\rm H2O2}$ is greater than 2 and varies from a value of 5 to 16. Φ_H and Φ_{H2O2} also differ significantly among the samples, from a value of 1.7–17 \times 10^{-4} for Φ_H and 0.21–1.03 \times 10^{-4} for Φ_{H2O2} . Literature values for polychromatic Φ_{H2O2} values for a variety of natural waters vary significantly. ^{21,23,47,52} Our results are on the lower end of published values, which could be due to the differences in experimental methods as described above (wavelength of cutoff filter and integrated wavelength range).

 $R_{\rm H}/R_{\rm H2O2}$ values for SRFA and SRNOM are comparable to one another and to previously published results for SRFA and

Table 1. $R_{\rm H}$ and $R_{\rm H2O2}$, Apparent Quantum Yields, and Ratios for Various Samples^a

	D (35/)	D (35/)	D (35/) (434)	× (10-4)	± (12-4)	D /D	D (01)
sample	$R_{\rm H} ({\rm nM/s})$	$R_{\rm H2O2}~({\rm nM/s})$	$R_{\rm EX}~({\rm nM/s})~(\times~10^4)$	$\Phi_{\mathrm{H}}~(imes~10^{-4})$	$\Phi_{\rm H2O2} \ (\times \ 10^{-4})$	$R_{\rm H}/R_{\rm H2O2}$	$P_{\rm O2-}~(\%)$
SRFA	20 ± 2	1.7 ± 0.1	2.3	9 ± 1	0.76 ± 0.05	12 ± 2	83
SRNOM	15 ± 1	1.4 ± 0.2	1.8	8.3 ± 0.8	0.8 ± 0.1	11 ± 2	81
ESHA	10.9 ± 0.5	0.74 ± 0.02	3.6	3.0 ± 0.1	0.21 ± 0.01	15 ± 1	86
Sargassum	6.4 ± 0.5	1.13 ± 0.03	3.8	1.7 ± 0.1	0.30 ± 0.008	5.7 ± 0.4	65
St. Nineteen (EX)	8.7 ± 0.3	0.67 ± 0.03	1.2	7.4 ± 0.3	0.58 ± 0.03	13.0 ± 0.8	85
St. Nineteen (NW)	5.3 ± 0.4	0.39 ± 0.02	0.61	8.6 ± 0.6	0.64 ± 0.03	13 ± 1	85
SMR (EX)	3.0 ± 0.3	0.21 ± 0.02	0.27	11 ± 1	0.75 ± 0.06	14 ± 2	86
SMR (NW)	2.1 ± 0.3	0.18 ± 0.01	0.22	10 ± 2	0.85 ± 0.05	11 ± 2	82
ECL (NW)	8.3 ± 0.4	0.661 ± 0.007	1.2	6.8 ± 0.3	0.544 ± 0.006	12.6 ± 0.5	84
GWL (NW)	4.7 ± 0.6	0.45 ± 0.01	0.61	8 ± 1	0.74 ± 0.02	11 ± 1	81
MKR (NW)	4.5 ± 0.6	0.277 ± 0.003	0.27	17 ± 2	1.03 ± 0.01	16 ± 2	88

^aUncertainties in the rates represent the standard deviation of triplicate measurements. Uncertainties were propagated for derived values.

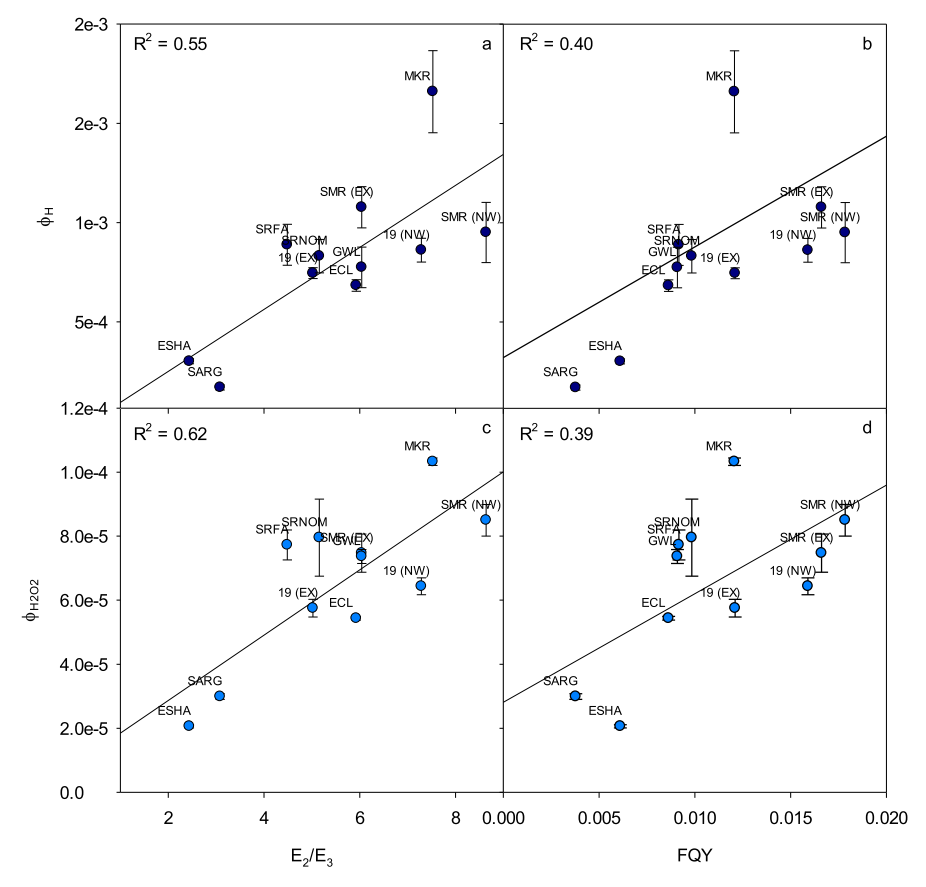


Figure 5. Relationships between optical properties and apparent quantum yields: (a) $\Phi_{\rm H}$ vs E_2/E_3 , (b) $\Phi_{\rm H}$ vs FQY, (c) $\Phi_{\rm H2O2}$ vs E_2/E_3 , and (d) $\Phi_{\rm H2O2}$ vs FQY for all samples given in Table 1. Error bars represent propagation of standard deviation of triplicate measurements.

SRHA.¹⁵ ESHA differs significantly from SRFA and SRNOM as it has a slightly higher $R_{\rm H}/R_{\rm H2O2}$ yet significantly lower $\Phi_{\rm H}$ and $\Phi_{\rm H2O2}$ values. The exudate from *Sargassum* is similar to ESHA in that $\Phi_{\rm H}$ and $\Phi_{\rm H2O2}$ are low compared to all of the other samples, however *Sargassum* has an overall $R_{\rm H}/R_{\rm H2O2}$ of 5 compared to 15 obtained for ESHA. This difference could be related to the fact that DOM from *Sargassum* exudates has a high phenolic content and very different molecular properties when compared to standard reference materials.³³ The natural waters and their respective extracts from St. Nineteen and SMR have fairly close values for both $\Phi_{\rm H}$ and $\Phi_{\rm H2O2}$. The natural water samples from New Jersey having varying values for both $\Phi_{\rm H}$ and $\Phi_{\rm H2O2}$. MKR has the highest $\Phi_{\rm H}$ and $\Phi_{\rm H2O2}$ values among the samples tested. Assuming that all of the

photoproduced OER that react with 3AP to produce hydroxylamine would react with molecular oxygen to produce superoxide, and assuming the stoichiometry of two superoxide molecules to produce one hydrogen peroxide, the fraction of superoxide that is lost to other oxidative processes ($P_{\rm O2-}$) can be determined using the following equation:¹⁵

$$\frac{R_{\rm H}}{R_{\rm H2O2}} = \frac{2R_{\rm O_2^-(total)}}{[R_{\rm O_2^-(total)}(1 - P_{\rm O_2^-(oxidative)})]} \tag{6}$$

The $P_{\rm O2-}$ (converted to percent) for the samples range from 65% to 88%, consistent with past results and suggesting that a significant portion of superoxide is lost through oxidative pathways. ^{15,19,22,56}

Table 2. Effect of Salinity and Addition of DTPA on $R_{\rm H}$ and $R_{\rm H2O2}$ in St. Nineteen EX and NW^a

sample	condition	$R_{\rm H}$ (nM/s)	$R_{\rm H2O2} (\rm nM/s)$	$R_{\rm H}/R_{\rm H2O2}$
St. Nineteen (EX)	none	8.7 ± 0.3	0.67 ± 0.03	13.0 ± 0.8
	18 ppt NaCl	6.7 ± 0.8	0.77 ± 0.03	9 ± 1
	28 ppt NaCl	8 ± 1	0.71 ± 0.05	11 ± 2
	18 ppt sea salt	7 ± 1	0.73 ± 0.09	9 ± 2
	28 ppt sea salt	6.7 ± 0.6	0.80 ± 0.01	8.4 ± 0.7
	50 μ M DTPA	8.8 ± 0.5	0.93 ± 0.03	9.3 ± 0.7
St. Nineteen (NW)	none	5.3 ± 0.4	0.39 ± 0.02	13 ± 1
	$50~\mu\mathrm{M}$ DTPA	5.5 ± 0.3	0.51 ± 0.02	10.6 ± 0.7

^aUncertainties in the rates represent the standard deviation of triplicate measurements. Uncertainties were propagated for derived values.

Comparison to Optical Properties. Variation in the Φ_{H} and Φ_{H2O2} values among the samples studied could be due to differences in structure or composition of the samples. Optical properties, such as absorbance and fluorescence parameters, have been utilized to relate photochemical reactions to the composition of CDOM.⁴ To probe this, several optical properties were obtained for the samples using absorbance and excitation-emission spectra. Φ_{H} and Φ_{H2O2} were compared to the ratio of the absorbance value at 250 nm to the absorbance value at 365 nm (E_2/E_3) , spectral slope $(S_{300-700})$, spectral slope ratio $(S_{275-295}/S_{350-400})$, and fluorescence quantum yield (FQY). A weak correlation was observed for $\Phi_{\rm H}$ and $\Phi_{\rm H2O2}$ with E_2/E_3 (R^2 = 0.55 and 0.62, respectively) and FQY (R^2 = 0.40 and 0.39, respectively) (Figure 5), but no obvious correlation was observed for Φ_H and $\Phi_{\rm H2O2}$ and $S_{300-700}$ or $S_{275-295}/S_{350-400}$ (Figure S18). $E_2/$ E_3 , $S_{300-700}$, $S_{275-295}/S_{350-400}$, and FQY all tend to increase with decreasing molecular weight, 4,57 so it is interesting that the correlations are stronger with some of these optical properties over others. It has been argued that the more discrete optical properties $(E_2/E_3$ and $S_{275-295}/S_{350-400})$ are more viable parameters to compare to as opposed to spectral slopes over broad wavelength regions because the analysis of a wide range of wavelengths would be less sensitive to any subtle changes in absorbance. However, our correlations to $S_{275-295}/S_{350-400}$ are minimal but this could be due to the very small range that the samples fall within (\sim 0.8-1.0) (Figure S18). Another aspect to note is that the E_2/E_3 includes the absorbance at 250 nm, whereas the spectral slope was calculated from 300 to 700 nm, indicating that the absorbance around 250 nm is of more importance than other wavelengths/regions when making correlations with Φ_{H} and Φ_{H2O2} .

On the basis of the correlations, it appears that $\Phi_{\rm H}$ and $\Phi_{\rm H2O2}$ also increase with decreasing molecular weight, although very little about these correlations exist in the literature. Dalrymple et al. found the opposite trend for $\Phi_{\rm H2O2}$ although their range in E_2/E_3 was considerably smaller than in our results. Their samples only consisted of extracts from the International Humic Substance Society, whereas our data set includes several natural waters. Furthermore, their quantum yields were based on the range of approximately 300–400 nm, whereas ours are calculated over the range of 300–800 nm. A linear relationship has been found between hydrogen peroxide production and fluorescence, in accordance with our results.

Effect of Salinity and Addition of Metal Chelators. Petasne and Zika calculated that the rate constant for dismutation of superoxide would decrease in seawater compared to pure water since cations found in seawater stabilize superoxide, increasing its lifetime and therefore decreasing $R_{\rm H2O2}$. Sodium chloride did not affect either

 $R_{\rm H}$ or $R_{\rm H2O2}$, but the presence of the sea salt seems to have slightly enhanced $R_{\rm H2O2}$ while possibly decreasing $R_{\rm H}$, although the $R_{\rm H}$ measurements are within the error of one another (Table 2). The increase in $R_{\rm H2O2}$ is the opposite of the work by Petasne and Zika although it is not a substantial increase. ¹⁹

Transition metals such as copper and iron are both commonly found in natural waters, typically in nanomolar concentrations. 61,62 Several works have demonstrated that copper and iron can catalyze the dismutation of superoxide with fairly high rate constants $(10^7 - 10^9 \text{ M}^{-1} \text{ s}^{-1})$, which would increase R_{H2O2} . 63-65 Alternatively, it has been shown that iron and copper can remove hydrogen peroxide through Fenton chemistry. 66-69 Superoxide has also been shown to reduce iron. These would all decrease the observed $R_{\rm H2O2}$. Metal chelators such as DTPA can chelate multiple metals including iron, copper, and manganese and make them unable to react.⁷³ DTPA itself, with or without complexed metals, has been shown to be unreactive or minimally reactive with superoxide due to its strong binding constants with metals. The addition of 50 μ M DTPA to both St. Nineteen extract and natural water had no impact on $R_{\rm H}$ and slightly increased $R_{\rm H2O2}$ for both samples (Table 2). The slightly increased values for $R_{\rm H2O2}$ results in lower ratios of $R_{\rm H}/R_{\rm H2O2}$ but the values are still much larger than 2. Therefore, the increase in $R_{\rm H2O2}$ in the presence of DTPA indicates that metals could be acting as a sink for superoxide, or even hydrogen peroxide, but it is not significant enough to account for the high $R_{\rm H}/R_{\rm H2O2}$ values. It is interesting that DTPA had the same effect on both the natural water and the extract. Due to the process of extraction, it is not expected that both the natural water and the extract would contain the same concentrations of metals. However, it has also been shown that metals that are strongly complexed with DOM can be retained during solid phase extraction using C-18 Sep-Pak and PPL resins. 75,76 Another chelator, desferrioxamine (DFOA), was also tested but due to its reaction with fluorescamine, was not explored further (Figure S19).

Possible Oxidative Superoxide Sinks. It has been previously proposed that superoxide could be lost to reaction with phenoxy radicals in CDOM that are generated during the one-electron transfer step since phenols could act as electron donors. 15,16,77 Electron donating capacity (EDC) and phenol content have been determined for reference materials previously and have been found to be correlated to one another. 78,79 SRFA and SRNOM have been found to have higher EDC and phenol content than ESHA which could explain why ESHA has much lower $\Phi_{\rm H}$ and $\Phi_{\rm H2O2}$ values than SRFA and SRNOM.

Work conducted on model compounds has shown that superoxide primarily undergoes addition with phenoxy radicals to form hydroperoxide structures which can undergo further reactions, the specifics of which depend on the structure of the phenol. 80-83 More recent studies on phenol transformation (tyrosine, acetaminophen, and 2,4,6-trimethylphenol), in the presence of humic substances, also found that the structure of the phenol dictated its transformation pathways.^{84,85} Additionally, the rate of transformation of tyrosine varied among the humic substances tested, 85 indicating the importance of the chemical structure of CDOM in this process. Interestingly, the photodegradation of the humic substance was inhibited in the presence of acetaminophen. 84 This result suggests that reaction between superoxide and external phenoxy radicals to induce their transformation interfered with the pathway of superoxide reacting with phenoxy radicals within DOM to induce its degradation.

■ ENVIRONMENTAL IMPORTANCE

Measurements of photoproduced OER were successfully performed using the newly improved fluorescence method on a wide variety of reference materials, natural waters, and extracts. The hydroxylamine method provides reasonable estimates for superoxide production and is faster and much easier to conduct than the traditional chemiluminescence superoxide method. This method should be amenable to continuous measurement via flow injection analysis, in a fashion similar to the chemiluminescence-based method for superoxide. The sensitivity should be sufficient enough for application to most fresh and coastal waters, and with longer irradiation times, to open ocean waters.

 $R_{\rm H}$, $R_{\rm O2\bullet-}$, and $R_{\rm H2O2}$ were measured on identical samples and under identical experimental conditions for the first time. All three rates displayed the same wavelength dependence, supporting a common origin for their formation as shown in Scheme 1. The large values obtained for $R_{\rm H}/R_{\rm H2O2}$ and for $R_{\rm O2 \bullet -}/R_{\rm H2O2}$ imply a significant oxidative sink for superoxide and verify that superoxide cannot be estimated simply from doubling hydrogen peroxide measurements. Phenoxy radicals could be a viable and substantial sink for superoxide due to their large rate constants of reaction. Subsequent reaction of this addition product has been shown to primarily lead to the loss of the parent phenol. This process could in part explain the transformation of terrestrial CDOM as it is transported to marine waters, which is currently a largely unknown process.

ASSOCIATED CONTENT

Supporting Information

The Supporting Information is available free of charge at https://pubs.acs.org/doi/10.1021/acs.est.1c04043.

Hydroxylamine standard curve, plots of various control experiments for hydroxylamine method, modifying hydroxylamine method for use in natural waters, hydrogen peroxide standard curve, signal vs time for the wavelength dependence of superoxide production, sample irradiance spectrum, oxidation of hydroxylamine with copper, reaction scheme for one-electron reductants and derivations of equations, other correlations between apparent quantum yields and optical properties, and derivatization of metal chelator desferrioxamine (PDF)

AUTHOR INFORMATION

Corresponding Author

Neil V. Blough – Department of Chemistry and Biochemistry, University of Maryland, College Park, Maryland 20742, *United States;* orcid.org/0000-0002-7938-4961; Email: neilb@umd.edu

Authors

Danielle M. Le Roux - Department of Chemistry and Biochemistry, University of Maryland, College Park, Maryland 20742, United States; o orcid.org/0000-0003-2849-6856

Leanne C. Powers - University of Maryland Center for Environmental Science, Chesapeake Biological Laboratory, Solomons, Maryland 20688, United States; o orcid.org/ 0000-0002-3538-7431

Complete contact information is available at: https://pubs.acs.org/10.1021/acs.est.1c04043

The authors declare no competing financial interest.

ACKNOWLEDGMENTS

This work was supported by grants from the NSF (OCE 1357411 and OCE 1924595). We thank Dr. Whitney King for his assistance with fixing our FeLume.

REFERENCES

- (1) Carlson, C. A.; Hansell, D. A. Chapter 3. DOM Sources, Sinks, Reactivity, and Budgets. In Biogeochemistry of Marine Dissolved Organic Matter, 2nd ed.; Academic Press: Boston, 2015; pp 65-126 DOI: 10.1016/B978-0-12-405940-5.00003-0.
- (2) Cooper, W. J.; Zika, R. G.; Petasne, R. G.; Fischer, A. M. Sunlight-Induced Photochemistry of Humic Substances in Natural Waters: Major Reactive Species. In Aquatic Humic Substances; Advances in Chemistry; American Chemical Society: Washington, DC, 1988; Vol. 219, pp 333-362 DOI: 10.1021/ba-1988-0219.ch022.
- (3) Kieber, D. J.; Peake, B. M.; Scully, N. M. Reactive Oxygen Species in Aquatic Ecosystems. In UV Effects in Aquatic Organisms and Ecosystems; Helbling, E. W., Zagarese, H., Eds.; The Royal Society of Chemistry: Cambridge, U.K., 2003; Vol. 1.
- (4) Sharpless, C. M.; Blough, N. V. The Importance of Charge-Transfer Interactions in Determining Chromophoric Dissolved Organic Matter (CDOM) Optical and Photochemical Properties. Environ. Sci. Process. Impacts 2014, 16 (4), 654.
- (5) Zepp, R. G.; Erickson, D. J., III; Paul, N. D.; Sulzberger, B. Interactive Effects of Solar UV Radiation and Climate Change on Biogeochemical Cycling. Photochem. Photobiol. Sci. 2007, 6 (3), 286.
- (6) Hansard, S. P.; Easter, H. D.; Voelker, B. M. Rapid Reaction of Nanomolar Mn(II) with Superoxide Radical in Seawater and Simulated Freshwater. Environ. Sci. Technol. 2011, 45 (7), 2811-
- (7) Voelker, B. M.; Sulzberger, B. Effects of Fulvic Acid on Fe(II) Oxidation by Hydrogen Peroxide. Environ. Sci. Technol. 1996, 30 (4),
- (8) Packer, J. L.; Werner, J. J.; Latch, D. E.; McNeill, K.; Arnold, W. A. Photochemical Fate of Pharmaceuticals in the Environment: Naproxen, Diclofenac, Clofibric Acid, and Ibuprofen. Aquat. Sci. 2003, 65 (4), 342–351.
- (9) Richard, C.; Canonica, S. Aquatic Phototransformation of Organic Contaminants Induced by Coloured Dissolved Natural Organic Matter. In Environmental Photochemistry Part II; Boule, P., Bahnemann, D. W., Robertson, P. K. J., Eds.; Springer-Verlag: Berlin/ Heidelberg, 2005; Vol. 2M, pp 299-323 DOI: 10.1007/b138187.

- (10) Felcyn, J. R.; Davis, J. C. C.; Tran, L. H.; Berude, J. C.; Latch, D. E. Aquatic Photochemistry of Isoflavone Phytoestrogens: Degradation Kinetics and Pathways. Environ. Sci. Technol. 2012, 46 (12), 6698-6704.
- (11) He, X.; Zhang, G.; de la Cruz, A. A.; O'Shea, K. E.; Dionysiou, D. D. Degradation Mechanism of Cyanobacterial Toxin Cylindrospermopsin by Hydroxyl Radicals in Homogeneous UV/H2O2 Process. Environ. Sci. Technol. 2014, 48 (8), 4495-4504.
- (12) Wang, X.; Wang, S.; Qu, R.; Ge, J.; Wang, Z.; Gu, C. Enhanced Removal of Chlorophene and 17β -Estradiol by Mn(III) in a Mixture Solution with Humic Acid: Investigation of Reaction Kinetics and Formation of Co-Oligomerization Products. Environ. Sci. Technol. 2018, 52 (22), 13222-13230.
- (13) Ossola, R.; Schmitt, M.; Erickson, P. R.; McNeill, K. Furan Carboxamides as Model Compounds To Study the Competition between Two Modes of Indirect Photochemistry. Environ. Sci. Technol. 2019, 53 (16), 9594-9603.
- (14) Del Vecchio, R.; Blough, N. V. On the Origin of the Optical Properties of Humic Substances. Environ. Sci. Technol. 2004, 38 (14), 3885-3891.
- (15) Zhang, Y.; Blough, N. V. Photoproduction of One-Electron Reducing Intermediates by Chromophoric Dissolved Organic Matter (CDOM): Relation to O $_2$ $^-$ and H $_2$ O $_2$ Photoproduction and CDOM Photooxidation. Environ. Sci. Technol. 2016, 50 (20), 11008-
- (16) Zhang, Y.; Del Vecchio, R.; Blough, N. V. Investigating the Mechanism of Hydrogen Peroxide Photoproduction by Humic Substances. Environ. Sci. Technol. 2012, 46 (21), 11836-11843.
- (17) Bielski, B. H. J.; Allen, A. O. Mechanism of the Disproportionation of Superoxide Radicals. J. Phys. Chem. 1977, 81
- (18) Bielski, B. H. J.; Cabelli, D. E.; Arudi, R. L.; Ross, A. B. Reactivity of HO2/O-2 Radicals in Aqueous Solution. J. Phys. Chem. Ref. Data 1985, 14 (4), 1041-1100.
- (19) Petasne, R.; Zika, R. G. Fate of Superoxide in Coastal Sea Water. Nature 1987, 325, 516-518.
- (20) Cudd, A.; Fridovich, I. Electrostatic Interactions in the Reaction Mechanism of Bovine Erythrocyte Superoxide Dismutase. I. Biol. Chem. 1982, 257 (19), 11443-11447.
- (21) Powers, L. C.; Miller, W. L. Apparent Quantum Efficiency Spectra for Superoxide Photoproduction and Its Formation of Hydrogen Peroxide in Natural Waters. Front. Mar. Sci. 2016, 3 DOI: 10.3389/fmars.2016.00235.
- (22) Garg, S.; Rose, A. L.; Waite, T. D. Photochemical Production of Superoxide and Hydrogen Peroxide from Natural Organic Matter. Geochim. Cosmochim. Acta 2011, 75 (15), 4310-4320.
- (23) Powers, L. C.; Miller, W. L. Blending Remote Sensing Data Products to Estimate Photochemical Production of Hydrogen Peroxide and Superoxide in the Surface Ocean. Environ. Sci. Process. Impacts 2014, 16 (4), 792-806.
- (24) Shaked, Y.; Harris, R.; Klein-Kedem, N. Hydrogen Peroxide Photocycling in the Gulf of Aqaba, Red Sea. Environ. Sci. Technol. 2010, 44 (9), 3238-3244.
- (25) Blough, N. V. Electron Paramagnetic Resonance Measurements of Photochemical Radical Production in Humic Substances. 1. Effects of Oxygen and Charge on Radical Scavenging by Nitroxides. Environ. Sci. Technol. 1988, 22 (1), 77-82.
- (26) Blough, N. V.; Simpson, D. J. Chemically Mediated Fluorescence Yield Switching in Nitroxide-Fluorophore Adducts: Optical Sensors of Radical/Redox Reactions. J. Am. Chem. Soc. 1988, 110 (6), 1915-1917.
- (27) Herbelin, S. E.; Blough, N. V. Intramolecular Quenching of Excited Singlet States in a Series of Fluorescamine- Derivatized Nitroxides. J. Phys. Chem. B 1998, 102 (42), 8170-8176.
- (28) Green, S. A.; Simpson, D. J.; Zhou, G.; Ho, P. S.; Blough, N. V. Intramolecular Quenching of Excited Singlet States by Stable Nitroxyl Radicals. J. Am. Chem. Soc. 1990, 112 (20), 7337-7346.

- (29) Kieber, D. J.; Blough, N. V. Determination of Carbon-Centered Radicals in Aqueous Solution by Liquid Chromatography with Fluorescence Detection. Anal. Chem. 1990, 62 (21), 2275-2283.
- (30) Kieber, D. J.; Blough, N. V. Fluorescence Detection of Carbon-Centered Radicals in Aqueous Solution. Free Radical Res. Commun. **1990**, 10 (1-2), 109-117.
- (31) Kieber, D. J.; Johnson, C. G.; Blough, N. V. Mass Spectrometric Identification of the Radical Adducts of a Fluorescamine-Derivatized Nitroxide. Free Radical Res. Commun. 1992, 16 (1), 35-39.
- (32) Johnson, C. G.; Caron, S.; Blough, N. V. Combined Liquid Chromatography/Mass Spectrometry of the Radical Adducts of a Fluorescamine-Derivatized Nitroxide. Anal. Chem. 1996, 68 (5), 867-
- (33) Powers, L. C.; Hertkorn, N.; McDonald, N.; Schmitt-Kopplin, P.; Del Vecchio, R.; Blough, N. V.; Gonsior, M. Sargassum Sp. Act as a Large Regional Source of Marine Dissolved Organic Carbon and Polyphenols. Global Biogeochem. Cycles 2019, 33 (11), 1423-1439.
- (34) Andrew, A. A.; Del Vecchio, R.; Zhang, Y.; Subramaniam, A.; Blough, N. V. Are Extracted Materials Truly Representative of Original Samples? Impact of C18 Extraction on CDOM Optical and Chemical Properties. Front. Chem. 2016, 4 DOI: 10.3389/ fchem.2016.00004.
- (35) Green, S. A.; Blough, N. V. Optical Absorption and Fluorescence Properties of Chromophoric Dissolved Organic Matter in Natural Waters. Limnol. Oceanogr. 1994, 39 (8), 1903-1916.
- (36) Dixon, M. The Acceptor Specificity of Flavins and Flavoproteins. I. Techniques for Anaerobic Spectrophotometry. Biochim. Biophys. Acta, Bioenerg. 1971, 226 (2), 241-258.
- (37) Stuever Kaltenbach, M.; Arnold, M. A. Acridinium Ester Chemiluminescence: PH Dependent Hydrolysis of Reagents and Flow Injection Analysis of Hydrogen Peroxide and Glutamate. Microchim. Acta 1992, 108 (3-6), 205-219.
- (38) Waterville Analytical Chemistries http://www. watervilleanalytical.com/chemistries.html (accessed 04/09/2018).
- (39) Miller, W. L.; Kester, D. R. Hydrogen Peroxide Measurement in Seawater by (p-Hydroxyphenyl)Acetic Acid Dimerization. Anal. Chem. 1988, 60 (24), 2711-2715.
- (40) Rose, A. L.; Moffett, J. W.; Waite, T. D. Determination of Superoxide in Seawater Using 2-Methyl-6-(4-Methoxyphenyl)-3,7-Dihydroimidazo [1,2-a] Pyrazin-3(7 H)-One Chemiluminescence. Anal. Chem. 2008, 80 (4), 1215-1227.
- (41) McDowell, M. S.; Bakac, A.; Espenson, J. H. A Convenient Route to Superoxide Ion in Aqueous Solution. Inorg. Chem. 1983, 22 (5), 847 - 848.
- (42) Anderson, J. H. The Copper-Catalysed Oxidation of Hydroxylamine. Analyst 1964, 89 (1058), 357.
- (43) Gomez, E.; Estela, J. M.; Cerda, V. Thermometric Determination of CuIIbased on Its Catalytic Effect on the Oxidation of Hydroxylamine by Dissolved Oxygen. Thermochim. Acta 1990, 165 (2), 255-260.
- (44) Green, S. A.; Morel, F. M. M.; Blough, N. V. Investigation of the Electrostatic Properties of Humic Substances by Fluorescence Quenching. Environ. Sci. Technol. 1992, 26 (2), 294-302.
- (45) King, D. W.; Cooper, W. J.; Rusak, S. A.; Peake, B. M.; Kiddle, J. J.; O'Sullivan, D. W.; Melamed, M. L.; Morgan, C. R.; Theberge, S. M. Flow Injection Analysis of H2O2 in Natural Waters Using Acridinium Ester Chemiluminescence: Method Development and Optimization Using a Kinetic Model. Anal. Chem. 2007, 79 (11), 4169-4176.
- (46) Sikorski, R. J.; Zika, R. G. Modeling Mixed-Layer Photochemistry of H 2 O 2: Optical and Chemical Modeling of Production. J. Geophys. Res. Oceans 1993, 98 (C2), 2315-2328.
- (47) Scully, N. M.; McQueen, D. J.; Lean, D. R. S. Hydrogen Peroxide Formation: The Interaction of Ultraviolet Radiation and Dissolved Organic Carbon in Lake Waters along a 43-75°N Gradient. Limnol. Oceanogr. 1996, 41 (3), 540-548.
- (48) Jerome, J. H.; Bukata, R. P. Impact of Stratospheric Ozone Depletion on Photoproduction of Hydrogen Peroxide in Lake Ontario. J. Great Lakes Res. 1998, 24 (4), 929-935.

- (49) Andrews, S. S.; Caron, S.; Zafiriou, O. C. Photochemical Oxygen Consumption in Marine Waters: A Major Sink for Colored Dissolved Organic Matter? *Limnol. Oceanogr.* **2000**, *45* (2), 267–277.
- (50) Yocis, B. H.; Kieber, D. J.; Mopper, K. Photochemical Production of Hydrogen Peroxide in Antarctic Waters. *Deep Sea Res.*, Part I 2000, 47 (6), 1077–1099.
- (51) Miller, W. L.; Moran, M.; Sheldon, W. M.; Zepp, R. G.; Opsahl, S. Determination of Apparent Quantum Yield Spectra for the Formation of Biologically Labile Photoproducts. *Limnol. Oceanogr.* **2002**, 47 (2), 343–352.
- (52) O'Sullivan, D. W.; Neale, P. J.; Coffin, R. B.; Boyd, T. J.; Osburn, C. L. Photochemical Production of Hydrogen Peroxide and Methylhydroperoxide in Coastal Waters. *Mar. Chem.* **2005**, *97* (1), 14–33.
- (53) Kieber, D. J.; Miller, G. W.; Neale, P. J.; Mopper, K. Wavelength and Temperature-Dependent Apparent Quantum Yields for Photochemical Formation of Hydrogen Peroxide in Seawater. *Environ. Sci. Process. Impacts* **2014**, *16* (4), 777–791.
- (54) Powers, L. C.; Miller, W. L. Hydrogen Peroxide and Superoxide Photoproduction in Diverse Marine Waters: A Simple Proxy for Estimating Direct CO ₂ Photochemical Fluxes: H ₂ O ₂ /O ₂ PROXY FOR CO ₂ PHOTOPRODUCTION. *Geophys. Res. Lett.* **2015**, 42 (18), 7696–7704.
- (55) Zhang, Y.; Simon, K. A.; Andrew, A. A.; Del Vecchio, R.; Blough, N. V. Enhanced Photoproduction of Hydrogen Peroxide by Humic Substances in the Presence of Phenol Electron Donors. *Environ. Sci. Technol.* **2014**, *48* (21), 12679–12688.
- (56) Powers, L. C.; Babcock-Adams, L. C.; Enright, J. K.; Miller, W. L. Probing the Photochemical Reactivity of Deep Ocean Refractory Carbon (DORC): Lessons from Hydrogen Peroxide and Superoxide Kinetics. *Mar. Chem.* **2015**, *177*, 306–317.
- (57) Helms, J. R.; Stubbins, A.; Ritchie, J. D.; Minor, E. C.; Kieber, D. J.; Mopper, K. Absorption Spectral Slopes and Slope Ratios as Indicators of Molecular Weight, Source, and Photobleaching of Chromophoric Dissolved Organic Matter. *Limnol. Oceanogr.* **2008**, *53* (3), 955–969.
- (58) Dalrymple, R. M.; Carfagno, A. K.; Sharpless, C. M. Correlations between Dissolved Organic Matter Optical Properties and Quantum Yields of Singlet Oxygen and Hydrogen Peroxide. *Environ. Sci. Technol.* **2010**, *44* (15), 5824–5829.
- (59) Bray, R. C.; Mautner, G. N.; Fielden, E. M.; Carle, C. I. Studies on the Superoxide Ion: Complex Formation with Barium and Calcium Ions Detected by EPR Spectroscopy and Kinetically. p 16.
- (60) Millero, F. J. Estimate of the Life Time of Superoxide in Seawater. Geochim. Cosmochim. Acta 1987, 51 (2), 351–353.
- (61) Buerge-Weirich, D.; Sulzberger, B. Formation of Cu(I) in Estuarine and Marine Waters: Application of a New Solid-Phase Extraction Method To Measure Cu(I). *Environ. Sci. Technol.* **2004**, 38 (6), 1843–1848.
- (62) Miller, W. L.; King, D. W.; Lin, J.; Kester, D. R. Photochemical Redox Cycling of Iron in Coastal Seawater. *Mar. Chem.* **1995**, *50* (1–4), 63–77.
- (63) Voelker, B. M.; Sedlak, D. L.; Zafiriou, O. C. Chemistry of Superoxide Radical in Seawater: Reactions with Organic Cu Complexes. *Environ. Sci. Technol.* **2000**, *34* (6), 1036–1042.
- (64) Zafiriou, O. C.; Voelker, B. M.; Sedlak, D. L. Chemistry of the Superoxide Radical (O2-) in Seawater: Reactions with Inorganic Copper Complexes. *J. Phys. Chem. A* **1998**, *102* (28), 5693–5700.
- (65) Heller, M. I.; Croot, P. L. Superoxide Decay Kinetics in the Southern Ocean. *Environ. Sci. Technol.* **2010**, 44 (1), 191–196.
- (66) White, E. M.; Vaughan, P. P.; Zepp, R. G. Role of the Photo-Fenton Reaction in the Production of Hydroxyl Radicals and Photobleaching of Colored Dissolved Organic Matter in a Coastal River of the Southeastern United States. *Aquat. Sci.* **2003**, *65* (4), 402–414.
- (67) Southworth, B. A.; Voelker, B. M. Hydroxyl Radical Production via the Photo-Fenton Reaction in the Presence of Fulvic Acid. *Environ. Sci. Technol.* **2003**, *37* (6), 1130–1136.

- (68) Moffett, J. W.; Zika, R. G. Measurement of Copper(I) in Surface Waters of the Subtropical Atlantic and Gulf of Mexico. *Geochim. Cosmochim. Acta* 1988, 52 (7), 1849–1857.
- (69) Pham, A. N.; Xing, G.; Miller, C. J.; Waite, T. D. Fenton-like Copper Redox Chemistry Revisited: Hydrogen Peroxide and Superoxide Mediation of Copper-Catalyzed Oxidant Production. *J. Catal.* **2013**, 301, 54–64.
- (70) Rose, A. L.; Waite, T. D. Role of Superoxide in the Photochemical Reduction of Iron in Seawater. *Geochim. Cosmochim. Acta* **2006**, 70 (15), 3869–3882.
- (71) Garg, S.; Rose, A. L.; Waite, T. D. Superoxide Mediated Reduction of Organically Complexed Iron(III): Comparison of Non-Dissociative and Dissociative Reduction Pathways. *Environ. Sci. Technol.* **2007**, *41* (9), 3205–3212.
- (72) Garg, S.; Rose, A. L.; Waite, T. D. Superoxide-Mediated Reduction of Organically Complexed Iron(III): Impact of PH and Competing Cations (Ca2+). *Geochim. Cosmochim. Acta* **2007**, 71 (23), 5620–5634.
- (73) Holloway, J. H.; Reilley, C. N. Metal Chelate Stability Constants of Aminopolycarboxylate Ligands. *Anal. Chem.* **1960**, 32 (2), 249–256.
- (74) Rose, A. L.; Waite, T. D. Reduction of Organically Complexed Ferric Iron by Superoxide in a Simulated Natural Water. *Environ. Sci. Technol.* **2005**, 39 (8), 2645–2650.
- (75) Elbaz-Poulichet, F.; Cauwet, G.; Guan, D. M.; Faguet, D.; Barlow, R.; Mantoura, R. F. C. C18 Sep-Pak Extractable Trace Metals in Waters from the Gulf of Lions. *Mar. Chem.* **1994**, *46* (1–2), *67*–75
- (76) Ksionzek, K. B.; Zhang, J.; Ludwichowski, K.-U.; Wilhelms-Dick, D.; Trimborn, S.; Jendrossek, T.; Kattner, G.; Koch, B. P. Stoichiometry, Polarity, and Organometallics in Solid-Phase Extracted Dissolved Organic Matter of the Elbe-Weser Estuary. *PLoS One* **2018**, 13 (9), e0203260.
- (77) Ma, J.; Nie, J.; Zhou, H.; Wang, H.; Lian, L.; Yan, S.; Song, W. Kinetic Consideration of Photochemical Formation and Decay of Superoxide Radical in Dissolved Organic Matter Solutions. *Environ. Sci. Technol.* **2020**, *54* (6), 3199–3208.
- (78) Aeschbacher, M.; Graf, C.; Schwarzenbach, R. P.; Sander, M. Antioxidant Properties of Humic Substances. *Environ. Sci. Technol.* **2012**, *46* (9), 4916–4925.
- (79) Walpen, N.; Schroth, M. H.; Sander, M. Quantification of Phenolic Antioxidant Moieties in Dissolved Organic Matter by Flow-Injection Analysis with Electrochemical Detection. *Environ. Sci. Technol.* **2016**, 50 (12), 6423–6432.
- (80) Jin, F.; Leitich, J.; von Sonntag, C. The Superoxide Radical Reacts with Tyrosine-Derived Phenoxyl Radicals by Addition Rather than by Electron Transfer. *J. Chem. Soc., Perkin Trans.* 2 **1993**, No. 9, 1592
- (81) Jonsson, M.; Lind, J.; Reitberger, T.; Eriksen, T. E.; Merenyi, G. Free Radical Combination Reactions Involving Phenoxyl Radicals. *J. Phys. Chem.* **1993**, 97 (31), 8229–8233.
- (82) d'Alessandro, N.; Bianchi, G.; Fang, X.; Jin, F.; Schuchmann, H.-P.; von Sonntag, C. Reaction of Superoxide with Phenoxyl-Type Radicals. J. Chem. Soc. Perkin Trans. 2 2000, No. 9, 1862–1867.
- (83) Winterbourn, C. C.; Kettle, A. J. Radical-Radical Reactions of Superoxide: A Potential Route to Toxicity. *Biochem. Biophys. Res. Commun.* **2003**, 305 (3), 729–736.
- (84) Chen, Y.; Zhang, X.; Feng, S. Contribution of the Excited Triplet State of Humic Acid and Superoxide Radical Anion to Generation and Elimination of Phenoxyl Radical. *Environ. Sci. Technol.* **2018**, *52* (15), 8283–8291.
- (85) Zhou, Q.; Zhang, X.; Zhou, C. Transformation of Amino Acid Tyrosine in Chromophoric Organic Matter Solutions: Generation of Peroxide and Change of Bioavailability. *Chemosphere* **2020**, 245, 125662.